CHALMERS

Chalmers Publication Library

Wave propagation of functionally graded layers treated by recursion relations and effective boundary conditions

This document has been downloaded from Chalmers Publication Library (CPL). It is the author´s version of a work that was accepted for publication in:

International Journal of Solids and Structures (ISSN: 0020-7683)

Citation for the published paper:
Golub, M. ; Boström, A. ; Folkow, P. (2013) "Wave propagation of functionally graded layers treated by recursion relations and effective boundary conditions". International Journal of Solids and Structures, vol. 50(5), pp. 766â772.

http://dx.doi.org/10.1016/j.ijsolstr.2012.11.003

Downloaded from: http://publications.lib.chalmers.se/publication/170248

Notice: Changes introduced as a result of publishing processes such as copy-editing and formatting may not be reflected in this document. For a definitive version of this work, please refer to the published source. Please note that access to the published version might require a subscription.

Chalmers Publication Library (CPL) offers the possibility of retrieving research publications produced at Chalmers University of Technology. It covers all types of publications: articles, dissertations, licentiate theses, masters theses, conference papers, reports etc. Since 2006 it is the official tool for Chalmers official publication statistics. To ensure that Chalmers research results are disseminated as widely as possible, an Open Access Policy has been adopted.
The CPL service is administrated and maintained by Chalmers Library.

(article starts on next page)

Wave propagation of functionally graded layers treated by recursion relations and effective boundary conditions

Mikhail V. Golub[a,b,*], Anders Boström[b], Peter D. Folkow[b]

[a] *Institute for Mathematics, Mechanics and Informatics, Kuban State University, Krasnodar, 350040 Russia*
[b] *Department of Applied Mechanics, Chalmers University of Technology, SE-412 96 Göteborg, Sweden*

Abstract

Wave propagation through a layer of a material that is inhomogeneous in the thickness direction, typically a functionally graded material (FGM), is investigated. The material parameters and the displacement components are expanded in power series in the thickness coordinate, leading to recursion relations among the displacement expansion functions. These can be used directly in a numerical scheme as a means to get good field representations when applying boundary conditions, and this can be done even if the layer is not thin. This gives a schema that is much more efficient than the approach of subdividing the layer into many sublayers with constant material properties. For thin layers for which the material parameter do not depend on the layer thickness the recursion relations can be used to eliminate all but the lowest order expansion functions. Employing the boundary conditions this leads to a set of effective boundary conditions relating the displacements and stresses

*Corresponding author
Email addresses: `m_golub@inbox.ru` (Mikhail V. Golub), `anders.bostrom@chalmers.se` (Anders Boström), `peter.folkow@chalmers.se` (Peter D. Folkow)

on the two sides of the layer, thus completely replacing the layer by these effective boundary conditions. Numerical examples illustrate the convergence properties of the scheme for FG layers and the influence of different variations of the material parameters in the FG layer.
Keywords: functionally graded materials, elastic waves, thin layer, interface, effective boundary conditions

---

1. Introduction

Wave propagation problems in layered media have been studied extensively in the literature. One particular field of interest concerns two homogeneous solids in contact, and especially how to model the interface boundary conditions properly. Usually perfect bonding is assumed implying continuity of stress and displacement across the interface. However, the actual interface is more complicated than that as it has properties different from the surroundings. This could either be at the micro level due to misfits at the grain boundaries, or on a larger scale where a thin interface layer connects the two solids, e.g. a glue. Various methods have been developed to model such imperfect bondings (Jones and Whittier, 1967; Rokhlin and Wang, 1991; Boström et al., 1992; Rokhlin and Huang, 1993). Another possible way of dealing with this mismatch between materials is to impose a layer of a functionally graded material in between the two homogeneous solids. Hereby the material properties vary continuously from one surface to another, which mitigates various interface problems such as delamination due to stress concentrations.

Functionally graded materials (FGM) are composite materials made of

two (or more) phases of material constituents, where the phase distribution varies continuously. The most used group of FGM consists of ceramic and metal phases. Such FGM were developed in the mid 1980s where the strength of the metal and the heat resistance of the ceramic made these materials well suited for high-temperature environments. FGM also possess a number of other advantages compared to homogeneous materials such as improved residual stress distribution, higher fracture toughness, and reduced stress intensity factors. Hence, FGM are nowadays used in many different fields of engineering (Birman and Byrd, 2007; Shen, 2009).

The amount of work on structural elements made of FGM is huge, comprising isotropic, anisotropic and piezoelectric functionally graded (FG) structures of all geometries. Considering flat layers (plates), dynamical problems on free FG plates have been much studied adopting the three-dimensional equation of motion as well as different approximate theories based on the Kirchhoff, Mindlin, and various higher order shear deformation assumptions (Reddy and Cheng, 2003; Vel and Batra, 2004; Matsunaga, 2008; Zhao et al., 2009; Cao et al., 2011). Coupling problems for FG plates placed between homogeneous layers have been less frequently investigated. Such work has recently been performed for sandwich panels in both statics (Kashtalyan and Menshykova., 2009) and dynamics (Li et al., 2008; Chehel Amirani et al., 2009; Hadji et al., 2011). The literature on transmission and reflection effects using FG layers is scarce. Results are presented in (Huang and Nutt, 2011) for the acoustic problem on a FG panel.

The present paper considers dynamic equations for an inhomogeneous layer placed between two other materials. The layer is typically an FG layer,

and is so designated in the following, but it may be any layer that is inhomogeneous in the thickness direction. The material parameters in the layer can vary in a more or less arbitrary way in the thickness direction although they are assumed continuous. However, they need not be continuous at the boundaries. In the following the surrounding materials are designated 'half-spaces', but this is certainly not necessary, they may be layered or inhomogeneous, or even a traction-free boundary is possible. The layer is modeled using the three-dimensional equations of motion where the material parameters and displacement components are expanded in power series in the thickness coordinate. This method has previously been used for other plate structures such as isotropic homogeneous plates (Boström et al., 2001), isotropic FG plates (Vel and Batra, 2004), anisotropic homogeneous plates (Mauritsson et al., 2011) and piezoelectric homogeneous plates (Johansson and Niklasson, 2003; Mauritsson et al., 2008; Mauritsson and Folkow, 2010). Insertion into the governing three-dimensional equations of motion results in recursion relations among the displacement expansion functions. For thicker layers or layers whose material properties depend on the layer thickness, these recursion relations can be used directly in a numerical scheme to get good field representations when applying boundary conditions. For thin layers for which the material parameters do not depend on the layer thickness the power series expansions in conjunction with these recursion relations are used in the continuity boundary conditions at the top and the bottom of the FG layer. By eliminating the internal layer fields, these boundary conditions are expressed in terms of the displacement and stress fields for the surrounding half-spaces. Hereby, the effects from the FG layer are replaced by effective boundary con-

ditions (containing tangential and time derivatives), expressed in terms of the exterior fields. It is thus not necessary to model and solve equations for the layer separately, which simplifies the analysis of such coupled problems. A similar approach has been used when deriving effective boundary conditions for homogeneous plates (Johansson et al., 2005) and porous plates (Folkow and Johansson, 2009) surrounded by fluid half-spaces, as well as for homogeneous piezoelectric layers bonded to elastic materials (Johansson and Niklasson, 2003; Mauritsson, 2009). The power series and the resulting effective boundary conditions can be truncated to arbitrary order in the thickness, resulting in a hierarchy of equations that from previous experience (Boström et al., 2001) are believed to be asymptotically correct also in the present case. Here, explicit results are presented including thickness terms of power four in the anti-plane (SH) case, and thickness terms of power two in the in-plane (P-SV) case. Also the fully three-dimensional effective boundary conditions are derived. Numerical results are presented for plane wave problems, where energy transmission coefficients are calculated using the recursion relations and different truncation orders of the displacement series expansions. When compared to the result from the exact three-dimensional equation of motion, the present theory is seen to converge as the truncation order is increased. Also the influence of different variations of the material parameters in the FG layer are investigated.

2. Anti-plane motion (SH case)

Consider first the simpler anti-plane (SH) case where the displacement has only one component. The geometry is specified in Fig. 1 which shows the

FG layer of thickness d and the surrounding two homogeneous half-spaces A ($z < 0$) and B ($z > d$). In the FG layer the density is $\rho(z)$ and the shear modulus is $\mu(z)$, where the z dependence is left arbitrary. In the half-spaces the material parameters are assumed to be constant and are denoted by a subscript A or B, thus the densities are ρ_A and ρ_B and the shear moduli are μ_A and μ_B. In Fig. 1 the boundary values of the displacement v and shear stress σ_{yz} in the two half-spaces are also indicated; these are the quantities that enter into the boundary conditions. In the FG layer the governing equation is

$$\frac{\partial \sigma_{yx}(x,z,t)}{\partial x} + \frac{\partial \sigma_{yz}(x,z,t)}{\partial z} = \rho(z)\frac{\partial^2 v(x,z,t)}{\partial t^2}, \tag{1}$$

where the two shear stresses are

$$\sigma_{yx}(x,z,t) = \mu(z)\frac{\partial v(x,z,t)}{\partial x}, \qquad \sigma_{yz}(x,z,t) = \mu(z)\frac{\partial v(x,z,t)}{\partial z}. \tag{2}$$

Accordingly the governing equation can be written in terms of the displacement

$$\frac{\partial}{\partial z}\left(\mu(z)\frac{\partial}{\partial z}\right) v(x,z,t) + \left(\mu(z)\frac{\partial^2}{\partial x^2} - \rho(z)\frac{\partial^2}{\partial t^2}\right) v(x,z,t) = 0. \tag{3}$$

To proceed the material parameters are expanded in power series

$$\rho(z) = \sum_{i=0}^{M} \rho_i z^i, \qquad \mu(z) = \sum_{i=0}^{M} \mu_i z^i. \tag{4}$$

The upper limit M depends on the model for the FG layer, in most cases a good enough representation should be obtained with low values on M. However, for the applicability of the present method the density and shear modulus need not be continuous at the boundaries between the FG layer

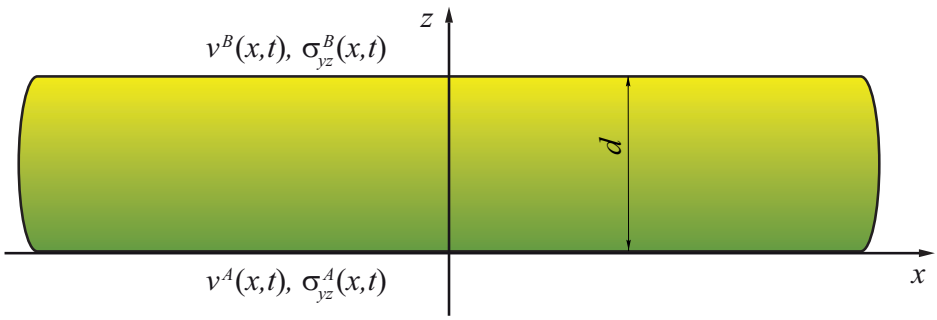

Figure 1: Geometry of the problem for an anti-plane motion of an FG layer with the boundary values of the displacements and stresses in the surrounding materials indicated.

and the half-spaces. Also the displacement in the FG layer is expanded in a power series

$$v(x,z,t) = \sum_{j=0}^{N} v_j(x,t) z^j, \tag{5}$$

where the expansion coefficients are thus functions of x and t. The upper limit must be chosen so that the results converge to a desired accuracy, and this is further discussed in the following and is investigated in the numerical examples. Substituting the power series expansions into Eq. 3 and putting each power of z to zero individually gives the following recursion relation

$$v_{k+2} = -\frac{1}{(k+1)(k+2)\mu_0}\left[\sum_{s=0}^{k} \mathcal{D}_s^T v_{k-s} + \sum_{s=1}^{k}(k-s+1)(k-s+2)\mu_s v_{k-s+2} + \sum_{s=0}^{k}(s+1)(k-s+1)\mu_{s+1} v_{k-s+1}\right], \quad k = 0,1,2,\ldots, \tag{6}$$

where the terms are written in terms of the horizontal shear wave operator

$$\mathcal{D}_s^T = -\rho_s \frac{\partial^2}{\partial t^2} + \mu_s \frac{\partial^2}{\partial x^2}, \quad s = 0,1,\ldots. \tag{7}$$

Accordingly, all the terms v_k, with $k = 2,3,\ldots$, can be expressed in terms of

v_0 and v_1, e.g.

$$v_2 = -\frac{1}{2\mu_0}\left[\mathcal{D}_0^T v_0 + \mu_1 v_1\right], \tag{8}$$

$$v_3 = -\frac{1}{6\mu_0^2}\left[\mu_0 \mathcal{D}_0^T v_1 + 2(\mu_0\mu_2 - \mu_1^2)v_1 + \mu_0 \mathcal{D}_1^T v_0 - 2\mu_1 \mathcal{D}_0^T v_0\right]. \tag{9}$$

The recursion relation can be used directly to obtain an accurate field representation in the layer which can be used when applying the boundary conditions. This works well also if the layer is not thin, but for thin layers one would expect that some sort of effective boundary conditions between the two half-spaces can be derived. In this way all effects of the layer are incorporated into the effective boundary conditions and the layer can be disregarded completely. However, if the material properties of the layer depend on the thickness of the layer this does not work as explained at the end of this section.

The boundary conditions at the boundaries of the FG layer are continuity of displacement and shear stress:

$$v(x,0,t) = v^A(x,t), \quad \sigma_{yz}(x,0,t) = \sigma_{yz}^A(x,t), \tag{10}$$

$$v(x,d,t) = v^B(x,t), \quad \sigma_{yz}(x,d,t) = \sigma_{yz}^B(x,t). \tag{11}$$

Here the limiting values of the displacement and stress in the two half-spaces $z < 0$ and $z > d$ are denoted by a superscript 'A' and 'B', respectively.

The boundary conditions at $z = 0$ directly give $v_0(x,t) = v^A(x,t)$ and $\mu_0 v_1(x,t) = \sigma_{yz}^A(x,t)$. Using this and the boundary conditions at $z = d$, and eliminating the expansion functions in the layer (v_0 and v_1), gives the effective boundary conditions between the two half-spaces A and B (taken at $z = 0$ and $z = d$, respectively):

$$v^B = v^A + \frac{d}{\mu_0}\sigma_{yz}^A - \frac{d^2}{2\mu_0^2}\left[\mu_0 \mathcal{D}_0^T v^A + \mu_1 \sigma_{yz}^A\right]$$

$$+\frac{d^3}{6\mu_0^3}\left[\mu_0\left(2\mu_1\mathcal{D}_0^T-\mu_0\mathcal{D}_1^T\right)v^A-\left(2\mu_0\mu_2-2\mu_1^2+\mu_0\mathcal{D}_0^T\right)\sigma_{yz}^A\right]$$
$$+\frac{d^4}{24\mu_0^4}\left[\mu_0\left(\mu_0\left(\mathcal{D}_0^T\right)^2-6\left(\mu_1^2-\mu_0\mu_2\right)\mathcal{D}_0^T+\mu_0\left(3\mu_1\mathcal{D}_1^T-2\mu_0\mathcal{D}_2^T\right)\right)v^A\right.$$
$$\left.-2\left(3\mu_1^3+3\mu_0^2\mu_3-6\mu_0\mu_1\mu_2-2\mu_0\mu_1\mathcal{D}_0^T+\mu_0^2\mathcal{D}_1^T\right)\sigma_{yz}^A\right], \quad (12)$$

$$\sigma_{yz}^B=\sigma_{yz}^A-d\mathcal{D}_0^Tv^A-\frac{d^2}{2\mu_0}\left[\mu_0\mathcal{D}_1^Tv^A+\mathcal{D}_0^T\sigma_{yz}^A\right]$$
$$+\frac{d^3}{6\mu_0^2}\left[\mu_0\left(\left(\mathcal{D}_0^T\right)^2-2\mu_0\mathcal{D}_2^T\right)v^A+\left(\mu_1\mathcal{D}_0^T-2\mu_0\mathcal{D}_1^T\right)\sigma_{yz}^A\right]$$
$$+\frac{d^4}{24\mu_0^3}\left[\mu_0\left(\mathcal{D}_0^T\right)^2-2\left(\mu_1^2-\mu_0\mu_2\right)\mathcal{D}_0^T+3\mu_0\left(\mu_1\mathcal{D}_1^T-2\mu_1\mathcal{D}_2^T\right)\sigma_{yz}^A\right.$$
$$\left.-2\mu_0\left(\mu_1\left(\mathcal{D}_0^T\right)^2-2\mu_0\mathcal{D}_1^T\mathcal{D}_0^T+3\mu_0^2\mathcal{D}_3^T\right)v^A\right]. \quad (13)$$

Here the x and t dependence of the field variables are suppressed. Terms up to order d^4 are included, but it is straightforward to include higher order terms also. However, if more terms are needed it is better to use the recursion relation repeatedly in the numerical scheme as explained above, and this is the procedure used when investigating the convergence numerically below.

The effective boundary conditions between the half-spaces are believed to be asymptotically correct to all orders in d, cf. Boström et al. (2001). However, for this to be true it is essential that the expansion coefficients of the material parameters ρ_i and μ_i are independent of d. Often, this will not be the case for FG layers. As an example, consider a linear variation inside the FG layer with the density and shear modulus continuous at the boundaries. Then $\mu_0=\mu_A$ and $\mu_1=(\mu_B-\mu_A)/d$ and similarly for the density. It is then easily seen that the d dependence of μ_1 destroys the asymptotic character of the boundary conditions; instead all terms will be of order d.

3. In-plane motion (P-SV case)

In the case of in-plane P-SV waves also the other Lamé constant λ is needed. It can depend on the z coordinate in the layer so $\lambda = \lambda(z)$. The displacement components in the x and z directions are u and w, respectively. The stresses expressed in the displacements are:

$$\sigma_{xz} = \mu(z)\left(\frac{\partial u}{\partial z} + \frac{\partial w}{\partial x}\right), \tag{14}$$

$$\sigma_{xx} = (\lambda(z) + 2\mu(z))\frac{\partial u}{\partial x} + \lambda(z)\frac{\partial w}{\partial z}, \tag{15}$$

$$\sigma_{zz} = \lambda(z)\frac{\partial u}{\partial x} + (\lambda(z) + 2\mu(z))\frac{\partial w}{\partial z}, \tag{16}$$

and the governing elastodynamic equations are

$$\frac{\partial}{\partial z}\left(\mu\frac{\partial u}{\partial z}\right) + (\lambda+\mu)\frac{\partial^2 w}{\partial x \partial z} + \frac{\partial \mu}{\partial z}\frac{\partial w}{\partial x} + (\lambda + 2\mu)\frac{\partial^2 u}{\partial x^2} - \rho\frac{\partial^2 u}{\partial t^2} = 0, \tag{17}$$

$$\frac{\partial}{\partial z}\left((\lambda+2\mu)\frac{\partial w}{\partial z}\right) + (\lambda+\mu)\frac{\partial^2 u}{\partial x \partial z} + \frac{\partial \lambda}{\partial z}\frac{\partial u}{\partial x} + \mu\frac{\partial^2 w}{\partial x^2} - \rho\frac{\partial^2 w}{\partial t^2} = 0. \tag{18}$$

The expansion of the Lamé constant λ is assumed in a power series

$$\lambda(z) = \sum_{i=0}^{M} \lambda_i z^i. \tag{19}$$

Also the displacements are expanded

$$u(x,z,t) = \sum_{j=0}^{N} u_j(x,t) z^j, \qquad w(x,z,t) = \sum_{j=0}^{N} w_j(x,t) z^j. \tag{20}$$

Introducing all series expansions into the governing equations and putting each power of z to zero individually leads to the recursion relations

$$u_{k+2} = -\frac{1}{(k+1)(k+2)\mu_0}\left[\sum_{s=1}^{k}(k-s+1)(k-s+2)\mu_s u_{k-s+2}\right.$$
$$+\sum_{s=0}^{k}\mathcal{D}_s^L u_{k-s} + \sum_{s=0}^{k}(s+1)(k-s+1)\mu_{s+1}u_{k-s+1}$$
$$\left.+\sum_{s=0}^{k}(s+1)\mu_{s+1}\mathcal{D}^x w_{k-s} + \sum_{s=0}^{k}(k-s+1)(\lambda_s+\mu_s)\mathcal{D}^x w_{k-s+1}\right], \qquad (21)$$

$$w_{k+2} = -\frac{1}{(k+1)(k+2)(\lambda_0+2\mu_0)}\left[\sum_{s=1}^{k}(k-s+1)(k-s+2)(\lambda_s+2\mu_s)w_{k-s+2}\right.$$
$$+\sum_{s=0}^{k}\mathcal{D}_s^T w_{k-s} + \sum_{s=0}^{k}(s+1)(k-s+1)(\lambda_{s+1}+2\mu_{s+1})w_{k-s+1}$$
$$\left.+\sum_{s=0}^{k}(s+1)\lambda_{s+1}\mathcal{D}^x u_{k-s} + \sum_{s=0}^{k}(k-s+1)(\lambda_s+\mu_s)\mathcal{D}^x u_{k-s+1}\right], \qquad (22)$$

where the new differential operators are

$$\mathcal{D}_s^L = -\rho_s\frac{\partial^2}{\partial t^2} + (\lambda_s+2\mu_s)\frac{\partial^2}{\partial x^2} \qquad s = 0, 1, \ldots, \qquad (23)$$

and

$$\mathcal{D}^x = \frac{\partial}{\partial x}. \qquad (24)$$

Applying all boundary conditions at $z = 0$ and $z = d$ leads to the effective boundary conditions between the half-spaces

$$u^B = u^A + d\left[\frac{1}{\mu_0}\sigma_{xz}^A - \mathcal{D}^x w^A\right]$$
$$-\frac{d^2}{2\mu_0}\left[\left(\mathcal{D}_0^L - \frac{\lambda_0(\lambda_0+\mu_0)}{\lambda_0+2\mu_0}(\mathcal{D}^x)^2\right)u^A + \frac{\mu_1}{\mu_0}\sigma_{xz}^A + \frac{\lambda_0+\mu_0}{\lambda_0+2\mu_0}\mathcal{D}^x\sigma_{zz}^A\right], \qquad (25)$$

$$
\begin{aligned}
w^B = w^A + d\left[\frac{\sigma_{zz}^A - \lambda_0 \mathcal{D}^x u^A}{\lambda_0 + 2\mu_0}\right] \\
+\frac{d^2}{2(\lambda_0+2\mu_0)}\Big[\left((\lambda_0+\mu_0)(\mathcal{D}^x)^2 - \mathcal{D}_0^T\right) w^A \\
+2\frac{\mu_1\lambda_0 - \mu_0\lambda_1}{(\lambda_0+2\mu_0)}\mathcal{D}^x u^A - \frac{\lambda_0+\mu_0}{\mu_0}\mathcal{D}^x\sigma_{xz}^A - \frac{\lambda_1+2\mu_1}{\lambda_0+2\mu_0}\sigma_{zz}^A\Big],
\end{aligned} \tag{26}
$$

$$
\begin{aligned}
\sigma_{xz}^B = \sigma_{xz}^A + d\left[\left(\frac{\lambda_0^2}{\lambda_0+2\mu_0}(\mathcal{D}^x)^2 - \mathcal{D}_0^L\right)u^A - \frac{\lambda_0}{\lambda_0+2\mu_0}\mathcal{D}^x\sigma_{zz}^A\right] \\
-\frac{d^2}{2}\Bigg[\frac{\lambda_0(\lambda_0+\mu_0)(\mathcal{D}^x)^2 - (\lambda_0+2\mu_0)\mathcal{D}_0^L - \lambda_0\mathcal{D}_0^T}{(\lambda_0+2\mu_0)}\mathcal{D}^x w^A \\
+\left(\mathcal{D}_1^L - \lambda_0\frac{4\lambda_1\mu_0 + \lambda_0(\lambda_1 - 2\mu_1)}{(\lambda_0+2\mu_0)^2}(\mathcal{D}^x)^2\right)u^A \\
\left(-\frac{\lambda_0(\lambda_0+\mu_0)}{\mu_0(\lambda_0+2\mu_0)}(\mathcal{D}^x)^2 + \frac{1}{\mu_0}\mathcal{D}_0^L\right)\sigma_{xz}^A + 2\frac{\mu_0\lambda_1 - \mu_1\lambda_0}{(\lambda_0+2\mu_0)^2}\mathcal{D}^x\sigma_{zz}^A\Bigg],
\end{aligned} \tag{27}
$$

$$
\begin{aligned}
\sigma_{zz}^B = \sigma_{zz}^A + d\left[(\mu_0(\mathcal{D}^x)^2 - \mathcal{D}_0^T)w^A - \mathcal{D}^x\sigma_{xz}^A\right] \\
+\frac{d^2}{2}\Bigg[\left(\mathcal{D}_0^L + \frac{\lambda_0}{\lambda_0+2\mu_0}\mathcal{D}_0^T - \frac{\lambda_0(\lambda_0+\mu_0)}{\lambda_0+2\mu_0}(\mathcal{D}^x)^2\right)\mathcal{D}^x u^A \\
+\left(\mu_1(\mathcal{D}^x)^2 - \mathcal{D}_1^L\right)w^A + \frac{\lambda_0+\mu_0}{\lambda_0+2\mu_0}(\mathcal{D}^x)^2\sigma_{zz}^A + \frac{1}{\lambda_0+2\mu_0}\mathcal{D}_0^T\sigma_{zz}^A\Bigg],
\end{aligned} \tag{28}
$$

where a superscript 'A' or 'B' again denotes the limiting value from the half-spaces. The x and t dependence of the fields are again not written out explicitly. These effective boundary conditions are only given to second order in d, the higher order terms become very complicated. The same remarks are valid for these conditions as for the corresponding SH conditions.

4. Three-dimensional case

Turning to the fully three-dimensional case, the governing elastodynamic equations of motion are

$$\frac{\partial}{\partial z}\left(\mu\frac{\partial u}{\partial z}\right)+(\lambda+\mu)\frac{\partial^2 w}{\partial x\partial z}+\frac{\partial\mu}{\partial z}\frac{\partial w}{\partial x}+(\lambda+\mu)\frac{\partial^2 v}{\partial x\partial y}$$
$$+(\lambda+2\mu)\frac{\partial^2 u}{\partial x^2}+\mu\frac{\partial^2 u}{\partial y^2}-\rho\frac{\partial^2 u}{\partial t^2}=0, \qquad (29)$$
$$\frac{\partial}{\partial z}\left(\mu\frac{\partial v}{\partial z}\right)+\frac{\partial\mu}{\partial z}\frac{\partial w}{\partial y}+(\lambda+\mu)\frac{\partial^2 w}{\partial y\partial z}+(\lambda+\mu)\frac{\partial^2 u}{\partial x\partial y}$$
$$+\mu\frac{\partial^2 v}{\partial x^2}+(\lambda+2\mu)\frac{\partial^2 v}{\partial y^2}-\rho\frac{\partial^2 v}{\partial t^2}=0, \qquad (30)$$
$$\frac{\partial}{\partial z}\left((\lambda+2\mu)\frac{\partial w}{\partial z}\right)+(\lambda+\mu)\left(\frac{\partial^2 u}{\partial x\partial z}+\frac{\partial^2 v}{\partial y\partial z}\right)+\frac{\partial\lambda}{\partial z}\frac{\partial u}{\partial x}+\frac{\partial\lambda}{\partial z}\frac{\partial v}{\partial y}$$
$$+\mu\frac{\partial^2 w}{\partial x^2}+\mu\frac{\partial^2 w}{\partial y^2}-\rho\frac{\partial^2 w}{\partial t^2}=0, \qquad (31)$$

where the same notions as earlier are used. The density, the Lamé constants, and the displacement components are expanded in power series exactly as in previous sections, and this leads to the following recursion relations

$$u_{k+2}=-\frac{1}{(k+1)(k+2)\mu_0}\left[\sum_{s=1}^{k}(k-s+1)(k-s+2)\mu_s u_{k-s+2}\right.$$
$$+\sum_{s=0}^{k}\mathcal{D}_s^1 u_{k-s}+\sum_{s=0}^{k}(s+1)(k-s+1)\mu_{s+1}u_{k-s+1}+\sum_{s=0}^{k}(s+1)\mu_{s+1}\mathcal{D}^x w_{k-s}$$
$$\left.+\sum_{s=0}^{k}(k-s+1)(\lambda_s+\mu_s)\mathcal{D}^x w_{k-s+1}+\sum_{s=0}^{k}(\lambda_s+\mu_s)\mathcal{D}^x\mathcal{D}^y v_{k-s}\right], \qquad (32)$$

$$v_{k+2}=-\frac{1}{(k+1)(k+2)\mu_0}\left[\sum_{s=1}^{k}(k-s+1)(k-s+2)\mu_s v_{k-s+2}\right.$$
$$+\sum_{s=0}^{k}\mathcal{D}_s^2 v_{k-s}+\sum_{s=0}^{k}(s+1)(k-s+1)\mu_{s+1}v_{k-s+1}+\sum_{s=0}^{k}(s+1)\mu_{s+1}\mathcal{D}^y w_{k-s}$$

$$+\sum_{s=0}^{k}(k-s+1)(\lambda_s+\mu_s)\mathcal{D}^y w_{k-s+1}+\sum_{s=0}^{k}(\lambda_s+\mu_s)\mathcal{D}^x\mathcal{D}^y u_{k-s}\Bigg],\quad(33)$$

$$\begin{aligned}w_{k+2}=-\frac{1}{(k+1)(k+2)(\lambda_0+2\mu_0)}\Bigg[&\sum_{s=1}^{k}(k-s+1)(k-s+2)(\lambda_s+2\mu_s)w_{k-s+2}\\&+\sum_{s=0}^{k}\mathcal{D}_s^3 w_{k-s}+\sum_{s=0}^{k}(s+1)(k-s+1)(\lambda_{s+1}+2\mu_{s+1})w_{k-s+1}\\&+\sum_{s=0}^{k}(s+1)\lambda_{s+1}(\mathcal{D}^x u_{k-s}+\mathcal{D}^y v_{k-s})\\&+\sum_{s=0}^{k}(k-s+1)(\lambda_s+\mu_s)(\mathcal{D}^x u_{k-s+1}+\mathcal{D}^y v_{k-s+1})\Bigg].\quad(34)\end{aligned}$$

Here the differential operators are

$$\mathcal{D}_s^1=\left((\lambda_s+2\mu_s)\frac{\partial^2}{\partial x^2}+\mu_s\frac{\partial^2}{\partial y^2}-\rho_s\frac{\partial^2}{\partial t^2}\right),\quad(35)$$

$$\mathcal{D}_s^2=\left(\mu_s\frac{\partial^2}{\partial x^2}+(\lambda_s+2\mu_s)\frac{\partial^2}{\partial y^2}-\rho_s\frac{\partial^2}{\partial t^2}\right),\quad(36)$$

$$\mathcal{D}_s^3=\left(\mu_s\frac{\partial^2}{\partial x^2}+\mu_s\frac{\partial^2}{\partial y^2}-\rho_s\frac{\partial^2}{\partial t^2}\right),\quad(37)$$

where $s=0,1,\ldots$, and

$$\mathcal{D}^x=\frac{\partial}{\partial x},\quad \mathcal{D}^y=\frac{\partial}{\partial y}.\quad(38)$$

Applying all boundary conditions at $z=0$ and $z=d$ finally leads to the effective boundary conditions between the half-spaces

$$\begin{aligned}u^B=u^A+d\left[\frac{1}{\mu_0}\sigma_{xz}^A-\mathcal{D}^x w^A\right]\\-\frac{d^2}{2\mu_0}\left[\left(\mathcal{D}_0^1-\frac{\lambda_0(\lambda_0+\mu_0)}{\lambda_0+2\mu_0}(\mathcal{D}^x)^2\right)u^A+2\mu_0\frac{\lambda_0+\mu_0}{\lambda_0+2\mu_0}\mathcal{D}^x\mathcal{D}^y v^A+\frac{\mu_1}{\mu_0}\sigma_{xz}^A+\frac{\lambda_0+\mu_0}{\lambda_0+2\mu_0}\mathcal{D}^x\sigma_{zz}^A\right],\quad(39)\end{aligned}$$

$$v^B = v^A + d\left[\frac{1}{\mu_0}\sigma^A_{yz} - \mathcal{D}^y w^A\right]$$
$$-\frac{d^2}{2\mu_0}\left[\left(\mathcal{D}^2_0 - \frac{\lambda_0(\lambda_0+\mu_0)}{\lambda_0+2\mu_0}(\mathcal{D}^y)^2\right)v^A + 2\mu_0\frac{\lambda_0+\mu_0}{\lambda_0+2\mu_0}\mathcal{D}^x\mathcal{D}^y u^A + \frac{\mu_1}{\mu_0}\sigma^A_{yz} + \frac{\lambda_0+\mu_0}{\lambda_0+2\mu_0}\mathcal{D}^y\sigma^A_{zz}\right], \quad (40)$$

$$w^B = w^A + d\left[\frac{\sigma^A_{zz} - \lambda_0(\mathcal{D}^x u^A + \mathcal{D}^y v^A)}{\lambda_0+2\mu_0}\right]$$
$$+\frac{d^2}{2}\left[\frac{(\lambda_0+\mu_0)\left((\mathcal{D}^x)^2 + (\mathcal{D}^y)^2\right) - \mathcal{D}^3_0}{(\lambda_0+2\mu_0)}w^A\right.$$
$$\left.+2\frac{\mu_1\lambda_0 - \mu_0\lambda_1}{(\lambda_0+2\mu_0)^2}\left(\mathcal{D}^x u^A + \mathcal{D}^y v^A\right) - \frac{\lambda_0+\mu_0}{\mu_0(\lambda_0+2\mu_0)}\left(\mathcal{D}^x\sigma^A_{xz} + \mathcal{D}^y\sigma^A_{yz}\right) - \frac{\lambda_1+2\mu_1}{(\lambda_0+2\mu_0)^2}\sigma^A_{zz}\right], \quad (41)$$

$$\sigma^B_{xz} = \sigma^A_{xz} + d\left[\left(\frac{\lambda_0^2}{\lambda_0+2\mu_0}(\mathcal{D}^x)^2 - \mathcal{D}^1_0\right)u^A - \frac{\mu_0(3\lambda_0+2\mu_0)}{\lambda_0+2\mu_0}\mathcal{D}^x\mathcal{D}^y v^A - \frac{\lambda_0}{\lambda_0+2\mu_0}\mathcal{D}^x\sigma^A_{zz}\right]$$
$$-\frac{d^2}{2}\left[\frac{\lambda_0(\lambda_0+\mu_0)(\mathcal{D}^x)^2 - \mu_0(\lambda_0+\mu_0)(\mathcal{D}^y)^2 - (\lambda_0+2\mu_0)\mathcal{D}^1_0 - \lambda_0\mathcal{D}^3_0}{(\lambda_0+2\mu_0)}\mathcal{D}^x w^A\right.$$
$$+\left(\mathcal{D}^1_1 - \frac{\lambda_0(4\lambda_1\mu_0 + \lambda_0(\lambda_1 - 2\mu_1))}{(\lambda_0+2\mu_0)^2}(\mathcal{D}^x)^2\right)u^A + \frac{4\lambda_1\mu_0^2 + \mu_1(3\lambda_0^2 + 4\lambda_0\mu_0 + 4\mu_0^2)}{(\lambda_0+2\mu_0)^2}\mathcal{D}^x\mathcal{D}^y v^A$$
$$\left.+\left(-\frac{\lambda_0(\lambda_0+\mu_0)}{\mu_0(\lambda_0+2\mu_0)}(\mathcal{D}^x)^2 + \frac{1}{\mu_0}\mathcal{D}^1_0\right)\sigma^A_{xz} + \frac{\mu_0+\lambda_0}{\lambda_0+2\mu_0}\mathcal{D}^x\mathcal{D}^y\sigma^A_{yz} + 2\frac{\mu_0\lambda_1 - \mu_1\lambda_0}{(\lambda_0+2\mu_0)^2}\mathcal{D}^x\sigma^A_{zz}\right], \quad (42)$$

$$\sigma^B_{yz} = \sigma^A_{yz} - d\left[\frac{\mu_0(3\lambda_0+2\mu_0)}{\lambda_0+2\mu_0}\mathcal{D}^x\mathcal{D}^y u^A + \left(-\frac{\lambda_0^2}{\lambda_0+2\mu_0}(\mathcal{D}^y)^2 + \mathcal{D}^2_0\right)v^A + \frac{\lambda_0}{\lambda_0+2\mu_0}\mathcal{D}^y\sigma^A_{zz}\right]$$
$$-\frac{d^2}{2}\left[\frac{\lambda_0(\lambda_0+\mu_0)(\mathcal{D}^y)^2 - 2\mu_0(\lambda_0+\mu_0)(\mathcal{D}^x)^2 - (\lambda_0+2\mu_0)\mathcal{D}^2_0 - \lambda_0\mathcal{D}^3_0}{\lambda_0+2\mu_0}\mathcal{D}^y w^A\right.$$
$$+\left(\mathcal{D}^2_1 - \frac{\lambda_0(4\lambda_1\mu_0 + \lambda_0(\lambda_1 - 2\mu_1))}{(\lambda_0+2\mu_0)^2}(\mathcal{D}^y)^2\right)v^A + \frac{4\lambda_1\mu_0^2 + \mu_1(3\lambda_0^2 + 4\lambda_0\mu_0 + 4\mu_0^2)}{(\lambda_0+2\mu_0)^2}\mathcal{D}^x\mathcal{D}^y u^A$$
$$\left.+\frac{\mu_0+\lambda_0}{\lambda_0+2\mu_0}\mathcal{D}^x\mathcal{D}^y\sigma^A_{xz} + \left(-\frac{\lambda_0(\lambda_0+\mu_0)}{\mu_0(\lambda_0+2\mu_0)}(\mathcal{D}^y)^2 + \frac{1}{\mu_0}\mathcal{D}^2_0\right)\sigma^A_{yz} + 2\frac{\mu_0\lambda_1 - \mu_1\lambda_0}{(\lambda_0+2\mu_0)^2}\mathcal{D}^y\sigma^A_{zz}\right], \quad (43)$$

$$
\begin{aligned}
\sigma_{zz}^B = \sigma_{zz}^A + d\left[(\mu_0((\mathcal{D}^x)^2 + (\mathcal{D}^y)^2) - \mathcal{D}_0^3)w^A - \mathcal{D}^y\sigma_{yz}^A - \mathcal{D}^x\sigma_{xz}^A\right] \\
+\frac{d^2}{2}\left[\left(\mathcal{D}_0^2 + \frac{2\mu_0(\lambda_0+\mu_0)(\mathcal{D}^x)^2 - \lambda_0(\lambda_0+\mu_0)(\mathcal{D}^y)^2 + \lambda_0\mathcal{D}_0^3}{\lambda_0+2\mu_0}\right)\mathcal{D}^y v^A\right. \\
\left(\mathcal{D}_0^1 + \frac{-\lambda_0(\lambda_0+\mu_0)(\mathcal{D}^x)^2 + 2\mu_0(\lambda_0+\mu_0)(\mathcal{D}^y)^2 + \lambda_0\mathcal{D}_0^3}{\lambda_0+2\mu_0}\right)\mathcal{D}^x u^A \\
\left.+(\mu_1((\mathcal{D}^x)^2 + (\mathcal{D}^y)^2) - \mathcal{D}_1^3)w^A + \frac{(\lambda_0+\mu_0)((\mathcal{D}^x)^2 + (\mathcal{D}^y)^2) - \mathcal{D}_0^3}{\lambda_0+2\mu_0}\sigma_{zz}^A\right]. \quad (44)
\end{aligned}
$$

As in the in-plane case the effective boundary conditions are written to second order in the thickness d. Comparing the three-dimensional case with the two two-dimensional ones it is apparent that the latter are special cases, exactly as they must be. As for the antiplane case the method is believed to be asymptotically correct to all orders, although this demands that the material parameters do not depend on the layer thickness.

5. Numerical examples

To validate the approach and to investigate the convergence a few numerical examples are now provided. An incoming plane wave from medium A is then assumed. This plane wave makes the angle θ_0 with the normal to the FG layer, and can be of SH, SV, or P type. These plane wave problems are then one- or two-dimensional, but this is not expected to influence the conclusions in the following. The transmission and reflection coefficients are calculated with the present approach. To this end a truncation N of the number of expansion coefficients (which in the case of plane waves are independent of x and t) in each displacement component is taken and the boundary conditions at $z = 0$ and $z = d$ are written down together with $N - 1$ recursion relations

for each displacement component. This yields a system of linear equations for the transmission and reflection coefficients and the displacement expansion coefficients which it is of course straightforward to solve. As a comparison the reflection and transmission problem is also solved by subdividing the FG layer into a (usually large) number of sublayers with constant material properties (Cretu and Nita, 2004; Wu et al., 2009). This method is straightforward and is not described further. It is checked that a sufficient number of layers are taken so the result has converged, see (Golub et al., 2012). In the following this method is designated the 'exact' one although it is not more exact than the method with the recursion relations, and generally speaking the method with sublayers is numerically much less effective. The number of sublayers needed varies with frequency, but typically up to 1000 layers are needed in the following computations.

The energy transmission coefficient and the energy reflection coefficient are used to characterize the transfer through the layer, where the total energy transmission coefficient, denoted κ^+, is the ratio of the time-averaged energy flow transmitted through the layer to the energy of the incident plane wave. Energy conservation can then be used as a check on the numerical computations.

Notation	Materials	Density $[kg/m^3]$	Young's modulus $[GPa]$	Poisson's ratio
A	Alumina	4000	400	0.231
B	Aluminium	2700	70	0.33

Table 1: Elastic moduli and densities of the half-spaces.

The variation of the material properties in the FG layer is assumed to be given by

$$P(z) = (P_B - P_A)\left(\frac{z}{d}\right)^M + P_A, \quad 0 < z < d. \tag{45}$$

Here $M = 1, 3$, or 5 is chosen, which means that the truncation of the expansion of the material parameters is also M. P is any of the parameters of the layer, i.e. ρ, μ, and λ are all assumed to have the same functional dependence on z. Note that the material parameters become continuous at the interface between the FG layer and the surrounding half-spaces. For $M = 1$ the dependence is linear and the parameters have a discontinuous derivative at the interfaces. For $M = 3$ and $M = 5$ the parameters have continuous derivatives at the interfaces.

In the numerical calculations the normalized frequency $\omega d/(2\pi c_B)$ is introduced, where d is the thickness of the FG layer and $c_B = \sqrt{\mu_B/\rho_B}$ is the shear wave velocity of material B. This dimensionless frequency thus measures the thickness of the FG layer in terms of the wavelength of material B (but with the material parameters chosen the wavelengths in the different materials are about the same). The two half-spaces are chosen as alumina and aluminium. The material properties used are specified in Table 1.

First a few examples are given to demonstrate the convergence of the scheme, varying the material law (the value of M), the type of incident wave, and the angle of incidence. Figure 2 shows the energy transmission coefficient for $M = 5$ and an SH wave with angle of incidence $\theta_0 = 0°$ and $\theta_0 = 15°$. A high truncation in N (the number of expansion terms for the displacement) is needed and it is also seen that a skew incidence needs a higher N than normal incidence; thus $N = 150$ is enough for normal incidence whereas $N = 200$ is

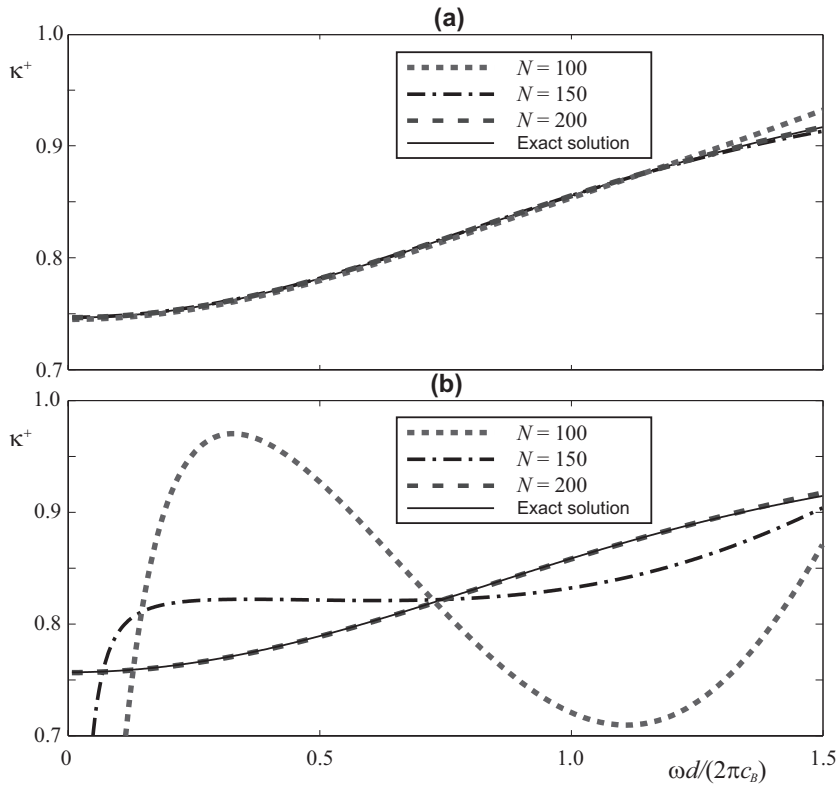

Figure 2: Energy transmission coefficient κ^+ for $M = 5$ and SH wave with $\theta_0 = 0°$(a) and $\theta_0 = 15°$(b).

needed for $\theta_0 = 15°$. Figure 3 likewise shows the convergence for $M = 3$ and an incident SV wave with $\theta_0 = 15°$. Here the even higher truncation $N = 250$ is needed to secure convergence. However, turning to the linear law $M = 1$ in Fig. 4, which is for an incoming P wave with $\theta_0 = 30°$, shows that in this case a much lower truncation is needed; it is in fact enough with $N = 40$. In conclusion it can be stated that moderate truncations, around $N = 40$, is enough for the linear law $M = 1$, whereas much higher truncations, around $N = 200$, are needed for the material laws with $M = 3$ and $M = 5$.

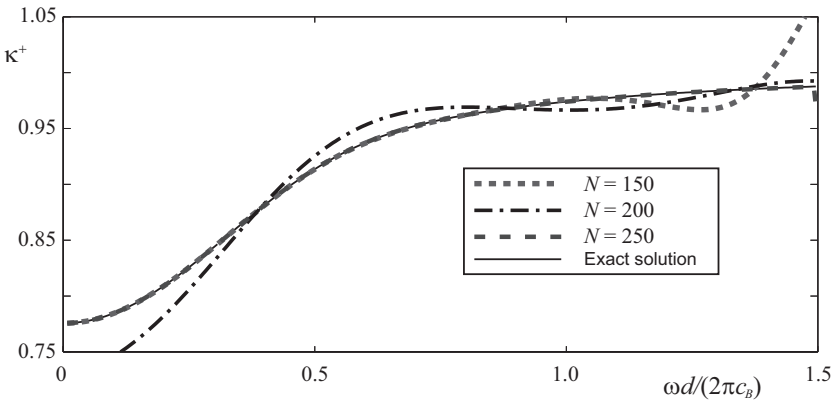

Figure 3: Energy transmission coefficient κ^+ for $M = 3$ and SV wave with $\theta_0 = 15°$.

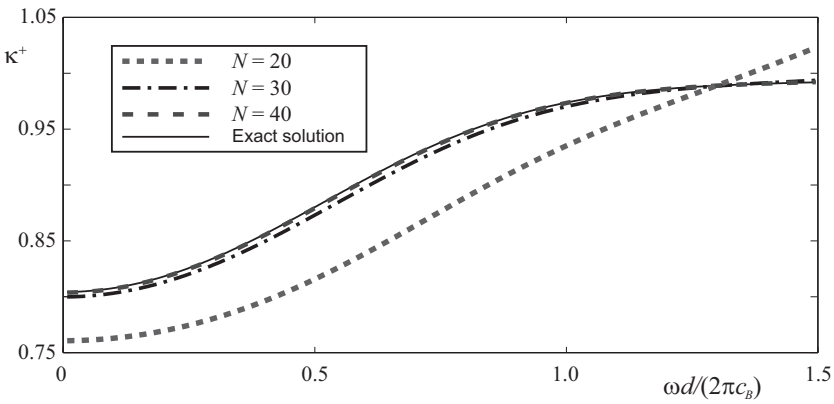

Figure 4: Energy transmission coefficient κ^+ for $M = 1$ and P wave with $\theta_0 = 30°$.

To investigate how important the variations of the material properties within a layer are, the three different laws $M = 1$, $M = 3$, and $M = 5$ are now compared with each other and also with the corresponding means. The means are of course calculated in the ordinary way, i.e.

$$\mu_0 = \frac{1}{d}\int_0^d \mu(z)\mathrm{d}z, \tag{46}$$

and similarly for λ and ρ. When using the means this also gives that $M = 0$

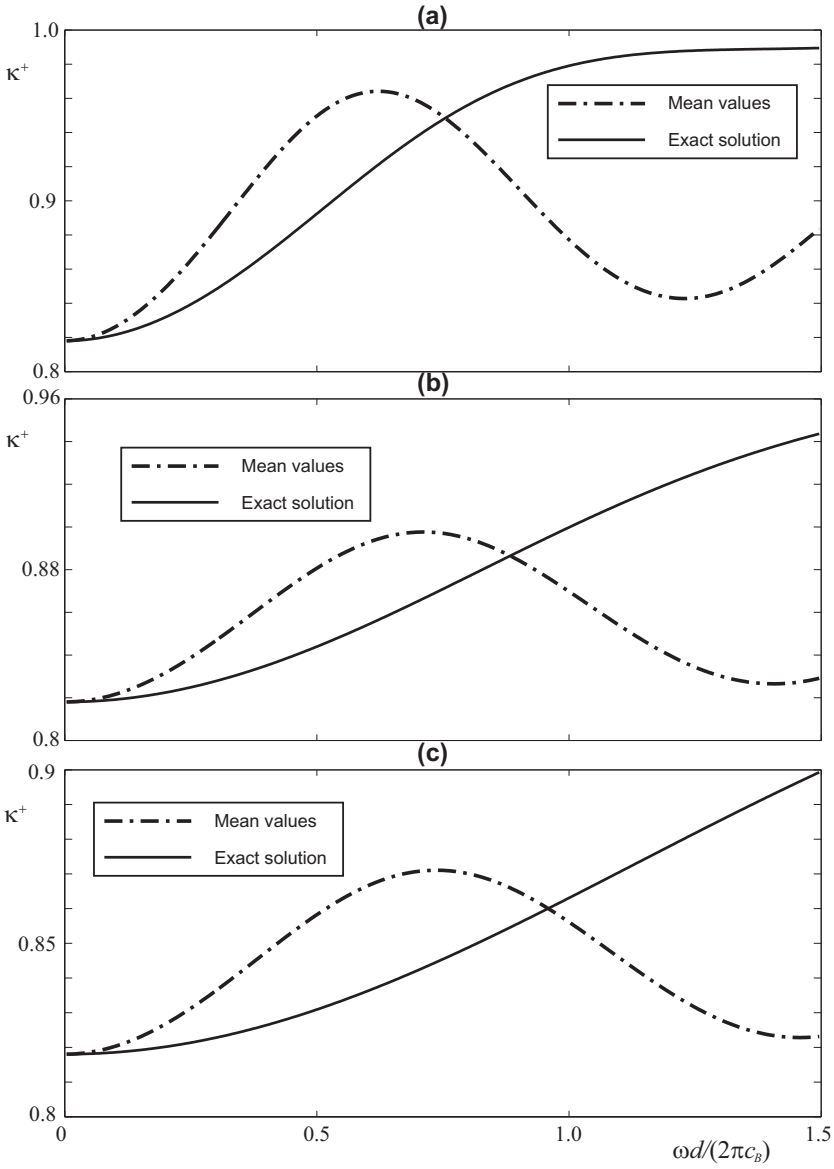

Figure 5: Energy transmission coefficient κ^+ for P wave with $\theta_0 = 45°$: mean value for elastic moduli (dash-dotted line) and exact solution (solid line). $M = 1$ (a); $M = 3$ (b); $M = 5$ (c).

can be used in the recursion relations. Figure 5 shows the energy transmission coefficient for an incoming P wave with $\theta_0 = 45°$ and the three M-values and the corresponding means. Note that all curves start at frequency $\omega = 0$ at $\kappa^+ = 0.818$, where the waves are so long so that there is no influence at all from the layer. When the frequency is increased all the six curves start to deviate from each other. It is noticed that the transmission for the means is larger than those for varying material parameters when the frequency is increasing from low values . Already around $\omega d/(2\pi c_B) = 0.05$ the deviations start, so already at this surprisingly low frequency the detailed material behaviour of the layer starts to be of importance.

6. Concluding remarks

It has been shown how the use of recursion relations for the displacement expansion functions is an effective way to treat a layer of an inhomogeneous material such as FGM. If the layer is thin and the material parameters in the layer do not depend on the layer thickness, the effective boundary conditions with only linear, or maybe quadratic, terms is an efficient way of treating the layer. If the material parameters depend on the layer thickness it is better to use the recursion relations directly in the numerical scheme, not making an analytical elimination of the expansion functions. This approach may also be good if the layer is thicker, and is more straightforward than replacing the layer by a (large) number of thin layers with constant material parameters or using some numerical scheme like FEM for the layer.

The number of expansion functions, and thereby the number of recursion relations, that are needed depend on exact material behaviour in the layer.

If powers higher than linear are used for the material behaviour, then a quite large number of expansion functions and recursion relations are needed. It even seems that the expansion can have divergence problems if $d^M \mu_M/\mu_0 > 1$, see Eq. 6, but this has not been further investigated, and it requires quite extreme material behaviour.

7. Acknowledgments

This joint research became possible thanks to the Swedish Institute. The authors are grateful to Professors E.V. Glushkov and N.V. Glushkova, and Dr. S.I. Fomenko for valuable discussions. The work is also supported by the Ministry of Education and Science of the Russian Federation (Project 14.B37.21.0387) and the Russian Foundation for Basic Research (Project 12-01-31001).

References

Birman, V., Byrd, L.W., 2007. Modeling and analysis of functionally graded materials and structures. Applied Mechanics Reviews 60, 195–216.

Boström, A., Bövik, P., Olsson, P., 1992. A comparison of exact first order and spring boundary conditions for scattering by thin layers. Journal of Nondestructive Evaluation 11, 175–184.

Boström, A., Johansson, G., Olsson, P., 2001. On the rational derivation of a hierarchy of dynamic equations for a homogeneous, isotropic, elastic plate. International Journal of Solids and Structures 38, 2487–2501.

Cao, X., Jin, F., Jeon, L., 2011. Calculation of propagation properties of Lamb waves in a functionally graded material (FGM) plate by power series technique. NDT & E International 44, 84–92.

Chehel Amirani, M., Khalili, S., Nemati, N., 2009. Free vibration analysis of sandwich beam with FG core using the element free Galerkin method. Composite Structures 90, 373–379.

Cretu, N., Nita, G., 2004. Pulse propagation in finite elastic inhomogeneous media. Journal of Sound and Vibration 222, 453–487.

Folkow, P.D., Johansson, M., 2009. Dynamic equations for fluid-loaded porous plates using approximate boundary conditions. Journal of the Acoustical Society of America 125, 2954–2966.

Golub, M.V., Fomenko, S. I., Bui, T. Q., Zhang, C., Wang, Y.-S., 2012. Transmission and band gaps of elastic SH waves in functionally graded periodic laminates. International Journal of Solids and Structures 49, 344–354.

Hadji, L., Atmane, H.A., Tounsi, A., Mechab, I., Adda Bedia, E.A., 2011. Free vibration of functionally graded sandwich plates using four-variable refined plate theory. Applied Mathematics and Mechanics 32, 925–942.

Huang, C., Nutt, S., 2011. An analytical study of sound transmission through unbounded panels of functionally graded materials. Journal of Sound and Vibration 330, 1153–1165.

Johansson, G., Niklasson, A.J., 2003. Approximate dynamic boundary conditions for a thin piezoelectric layer. International Journal of Solids and Structures 40, 3477–3492.

Johansson, M., Folkow, P.D., Hägglund, A.M., Olsson, P., 2005. Approximate boundary conditions for a fluid-loaded elastic plate. Journal of the Acoustical Society of America 118, 3436–3446.

Jones, J.P., Whittier, J.S., 1967. Waves in a flexibly bonded interface. Journal of Applied Mathematics and Mechanics 34, 905–909.

Kashtalyan, M., Menshykova., M., 2009. Three-dimensional elasticity solution for sandwich panels with a functionally graded core. Composite Structures 87, 36–43.

Li, Q., Iu, V., Kou, K., 2008. Three-dimensional vibration analysis of functionally graded material sandwich plates. Journal of Sound and Vibration 311, 498–515.

Matsunaga, H., 2008. Free vibration and stability of functionally graded plates according to a 2-D higher-order deformation theory. Composite Structures 82, 499 – 512.

Mauritsson, K., 2009. Modelling of finite piezoelectric patches: Comparing an approximate power series expansion theory with exact theory. International Journal of Solids and Structures 46, 1053–1065.

Mauritsson, K., Boström, A., Folkow, P.D., 2008. Modelling of thin piezoelectric layers on plates. Wave Motion 45, 616–628.

Mauritsson, K., Folkow, P.D., 2010. Dynamic equations for an orthotropic piezoelectric plate, in: Proceedings of the 10th International Conference on Computational Structures Technology, Valencia, pp. 1–14.

Mauritsson, K., Folkow, P.D., Boström, A., 2011. Dynamic equations for a fully anisotropic elastic plate. Journal of Sound and Vibration 330, 2640–2654.

Reddy, J.N., Cheng, Z.Q., 2003. Frequency of functionally graded plates with three-dimensional asymptotic approach. Journal of Engineering Mechanics 129, 896–900.

Rokhlin, S.I., Huang, W., 1993. Ultrasonic wave interaction with a thin anisotropic layer between two anisotropic solids: II Second-order asymptotic boundary conditions. Journal of the Acoustical Society of America 94, 3405–3420.

Rokhlin, S.I., Wang, Y.J., 1991. Analysis of boundary conditions for elastic wave interaction with an interface between two solids. Journal of the Acoustical Society of America 89, 503–515.

Shen, H.S., 2009. Functionally Graded Materials: Nonlinear Analysis of Plates and Shells. CRC Press Taylor & Francis Group, USA.

Vel, S.S., Batra, R.C., 2004. Three-dimensional exact solution for the vibration of functionally graded rectangular plates. Journal of Sound and Vibration 272, 703–730.

Wu, M.L., Wu, L.Y., Yang, W.P., Chen, L.W., 2009. Elastic wave band gaps

of one-dimensional phononic crystals with functionally graded materials. Smart Materials and Structures 18, 115013–.

Zhao, X., Lee, Y.Y., Liew, K.M., 2009. Free vibration analysis of functionally graded plates using the element-free kp-Ritz method. Journal of Sound and Vibration 319, 918–939.